Table I. Vapor Pressure of Solid 2,4-Hexadiyne[a]

t/°C	p/Torr	t/°C	p/Torr
0.00	0.5566	16.24	2.392
8.45	1.215	21.22	3.617
13.04	1.822		

[a] Antoine equation: $\log (p/\text{Torr}) = 10.34167 - 2706.727/(255.444 + t)$.

Table II. Vapor Pressure of Liquid 2,4-Hexadiyne[a]

t/°C	p/Torr	t_{water}/°C	t/°C	p/Torr	t_{water}/°C
91.991	229.98	69.615	103.832	344.93	79.267
98.925	293.52	75.350	112.047	450.86	85.995
107.526	390.17	82.327	116.678	520.55	89.729
119.026	559.37	91.631	121.785	607.09	93.824
124.557	658.92	96.049	129.032	749.03	99.593
130.706	785.82	100.939	135.444	895.34	104.658
95.303	259.03	72.384			

[a] Antoine equation: $\log (p/\text{Torr}) = 7.051846 - 1416.427/(210.006 + t)$. Cox equation: $\log (p/\text{atm}) = A' (1 - 402.688/T)$, where $\log A' = 0.830531 - 4.61921 \times 10^{-4} T + 3.07146 \times 10^{-7} T^2$.

were somewhat lower in temperature. Because of this uncertainty, we also measured the index of refraction of a very pure sample of naphthalene, obtained from Ambrose of NPL for use as a vapor pressure standard, under identical conditions.

Results

Results of the vapor pressure measurements are presented in Tables I and II, along with constants of appropriate correlating functions. There is definite curvature in $\ln p$ with $1/T$ for the solid, in spite of the narrow range of temperatures studied.

Data for the liquid include the temperature of the boiling water in equilibrium under the same helium pressure as the sample. The points are numbered chronologically, the first six measured on one day, and the last eight on the next. The sample was allowed to cool to room temperature overnight. Yellowing of the sample occurred on both days, and there is a trend in the deviations of the observed pressures from those produced by the correlating equations. It appears that a slight lowering of the pressure occurred over time, with the first day's data generally higher than, and the second day's lower than, the calculated values. No attempt was made to take this trend into account in the present work. The eighth point, being more than 3.5 standard deviations from its calculated value, was omitted in fitting equations to the data.

The indices of refraction of DMDA and naphthalene at a temperature near 87 °C are, respectively, 1.4760 and 1.5924.

Discussion

Cleveland et al. (*4*) report 129.51 ± 0.03 °C as the boiling point of DMDA, compared with the presently observed value, 129.54 °C. If the pressure were indeed dropping slightly with time, our value would be expected to be somewhat high.

The enthalpy of sublimation at 25 °C, under the assumption of vapor ideality, is 14.00 kcal/mol; extrapolation of the Cox equation under the same assumption provides 10.15 kcal/mol as the enthalpy of vaporization at 25 °C. Thus, the enthalpy of fusion would be 3.85 kcal/mol. Cleveland et al. (*4*) state that when heptane was used to depress the freezing point of DMDA, the lowering corresponded to 0.60 ± 0.03 °C/mol % impurity. Using the present value for enthalpy of fusion, and a melting point of 338.2 K, we calculate a freezing point depression constant of 0.590 °C/mol % impurity, in good agreement with the experimentally determined value.

The rodlike structure of DMDA might lead one to expect an elevated value for its Trouton's Rule constant; it is 22.63 cal/(mol K). This is a real effect, and is evidence for some degree of ordering in the liquid.

The triple point of the sample of DMDA used in the cooling curve analysis ($x = 0.9985$) was 64.87 °C; that of an absolutely pure sample would be 64.96 by this analysis, following Rossini (*5*). Cleveland and co-workers (*4*) report an "ultimate freezing point" of 65.08 °C; the difference (0.12 °C) is a real one, but may be partially accounted for by the effect of reduced pressure in lowering the triple point relative to the freezing point.

If we equate the expressions for solid and liquid vapor pressures we obtain the value 66.1 °C for the triple point. When the extent of extrapolation is considered, this is surprisingly close to the correct value. The vapor pressure at 64.96 °C calculated from the Cox equation is 79.9 Torr.

Registry No. DMDA, 2809-69-0.

Literature Cited

(1) Ambrose, D. *J. Sci. Instrum.* **1968**, 41.
(2) Meyer, E. F.; Hotz, R. D. *J. Chem. Eng. Data* **1973**, *18*, 359.
(3) Ambrose, D.; Sprake, C. H. S. *J. Chem. Thermodyn.* **1972**, 603.
(4) Cleveland, F. F.; Greenlee, K. W.; Bell, E. L. *J. Chem. Phys.* **1950**, *18*, 355.
(5) Rossini, F. D. *Chemical Thermodynamics*; Wiley: New York, 1950; pp 454-8.

Received for review September 13, 1985. Accepted December 16, 1985. Thanks are due Research Corporation for a grant to purchase the capacitance manometer used in this work. E.F.M. is grateful to the Chemistry Department of Texas Woman's University for hospitality and use of facilities during the analysis and write-up of this work.

FTIR Measurements of Solubilities of Anthracene in Supercritical CO_2

T. W. Zerda, B. Wiegand, and J. Jonas*
Department of Chemistry, University of Illinois, Urbana, Illinois 61801

The solubility of anthracene in carbon dioxide was measured at temperatures from 20 to 95 °C and at pressures up to 1200 bar. Anthracene concentrations were determined from the absorption in the IR region of anthracene C–H stretching vibrations. The results are compared with known literature data on solubilities of anthracene in CO_2. In addition, the observed frequency shift is discussed in terms of intermolecular interactions.

Introduction

During the past few years solvent extraction with supercritical fluids has become an important technological process. It has been used in decaffeinating coffee beans (*1*), regenerating activated carbon (*2*), deasphalting petroleum (*3*), separating organic chemicals from water (*4*), separating of a mixture of aromatic isomers (*5*), and in many other processes (*6*). In these extraction processes the effectiveness of the solvent is

0021-9568/86/1731-0274$01.50/0

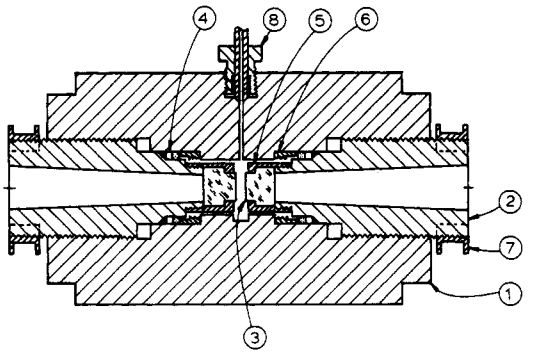

Figure 1. High-pressure stainless steel IR cell: 1, cell body; 2, plug; 3, sapphire window; 4, Bridgman rings; 5, window cup; 6, extraction ring; 7, electrical coil; 8, high-pressure tube with connection to the cell. Thermocouple inlet is perpendicular to the section shown.

characterized by solubility data of the solid. So far, most solubilities have been measured by using flow techniques (*7*, *8*). Two new methods have recently been developed in this laboratory, one involving NMR high-pressure experiments (*9*), and another using infrared absorption measurements. FTIR is especially well suited to determine solubilities in supercritical fluids because aromatic molecules have numerous IR active modes, and it is easy to find one or more characteristic bands well isolated from the solvent bands. The intensity of the solute band can be accurately determined, and from the Lambert–Beer law concentrations of solids can be found at various temperatures and pressures.

In this paper, we describe the FTIR technique and then present the results for the CO_2–anthracene system. Solubility data for anthracene are scarce; until now only two studies have been reported. Rossling and Franck (*10*) used UV absorption measurements and from peak intensities found solubilities of anthracene in numerous fluids (CO_2, NH_3, H_2O, CH_4, CHF_3, and others) at temperatures varying from 20 to 200 °C and pressures up to 2000 bar. Kwiatkowski et al. (*11*) used the flow technique and limited their study of anthracene in CO_2 to 40 °C and pressures ranging from 100 to 200 bar. Our results are compared to those reported in ref *10* and *11* and also presented in the form of the enhancement factor. This factor measures the extent to which a solvent enhances the solute concentration C as compared with the vapor concentration C^0 in equilibrium with the solid phase without the solvent.

Experimental Section

The concentration of a solute in a solution can be found from the intensity of the IR absorption band. Absorbance is given as $A = \ln I_0/I(\nu)$, where I_0 is the background and $I(\nu)$ is the intensity of the vibrational peak at frequency ν, and according to the Lambert–Beer law it is proportional to

$$A(\nu) = \epsilon(\nu)Cd \qquad (1)$$

C is the concentration of the sample in solution, d is the optical path length, and $\epsilon(\nu)$ is the absorption coefficient characteristic for the vibration band. For this study we concentrated on the C–H stretching vibration modes of anthracene located at about 3060 cm^{-1}. The molar absorption coefficient at the maximum of the 3060-cm^{-1} band was found to be ϵ = 180 L cm^{-1} mol^{-1} ± 10%. The detailed discussion of this value as well as how it has been determined is given in the next section.

All the experiments were performed using the FTIR Nicolet 9000 series spectrometer. Construction of the high-pressure IR cell built of stainless steel and equipped with cylindrical sapphire windows of diameter 18 mm and thickness 12 mm is based on that described in ref *12*. The windows were mounted

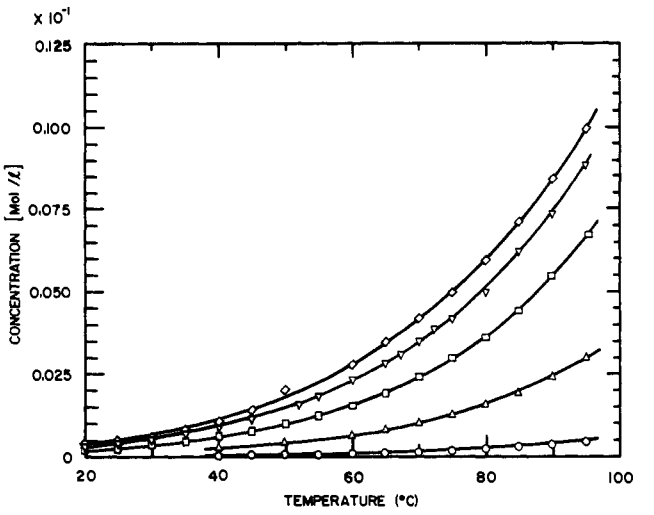

Figure 2. Solubilities of anthracene in CO_2 at different densities: ○, 0.294 kg/L; △, 0.643 kg/L; □, 0.803 kg/L; ▽, 0.876 kg/L; ◇, 1.001 kg/L.

on stainless steel plugs with a very thin indium foil spacer (5 μm). To allow measurements with the optical path length less than 1 mm, the windows were constructed in such a way that the window cups were completely hidden and did not protrude above the window surface (see Figure 1). The distance between the windows could be changed from 0.2 to 16 mm by using Bridgman type O-rings of different length. The optical path length was determined to within ±0.03 mm.

Temperature was measured by using a thermocouple located within the sample cell. Temperature was regulated by circulating fluid through the heating jacket surrounding the cell. Although the windows are located well inside the cell (Figure 1), we found that their surface temperature was slightly lower (up to 3 °C) than that of the cell. Thus, in order to prevent deposition of vapor anthracene on the cooler windows, the windows were heated by electrical coils mounted on the plugs.

Ultrapure CO_2 was purchased from Scientific Gas Product, Inc. This gas contained less than 1 ppm of hydrocarbons which absorb infrared radiation at frequencies from 3010 to 2850 cm^{-1}, below the region where anthracene C–H bands are located. Prior to the main experiment, the absorption spectra of CO_2 were recorded at all of the studied temperatures and pressures. These spectra were later carefully subtracted from the overall band shape of anthracene–CO_2 mixtures.

Several pieces of anthracene crystals were inserted through the thermocouple opening and were placed in a shallow dent in the bottom of the cell well below the light beam. To avoid contamination with water and atmospheric gases, the system (membrane compressor, tubings, valves, and the cell) was purged with CO_2 and later vacuum pumped. Spectra were recorded and stored only after the solubility equilibrium had been reached. This usually took 30 min, but in a few cases we waited from 8 to 12 h to be sure that equilibrium had been reached. Pressure was determined within 0.5 bar and temperature was stabilized to better than ±0.2 °C. The densities of CO_2 at various pressures and temperatures were calculated from the fifth-order polynomials found by the least-squares fitting routine to the density data published by Newitt et al. (*13*).

Results

The solubility data of the anthracene in carbon dioxide are listed in Table I (in mol L^{-1}) and Table II (in mole fraction), and some values are also plotted in Figure 2. The experimental error of the A/d ratio found by repeating the measurements 3 times, each with different optical path lengths, is less than 5%, but we estimate that the data in Table I are accurate only to

Table I. Solubilities of Anthracene in CO_2

density, kg L^{-1}	press., bar	temp, °C	solubility, mol L^{-1}	density, kg L^{-1}	press., bar	temp, °C	solubility, mol L^{-1}	density, kg L^{-1}	press., bar	temp, °C	solubility, mol L^{-1}
0.294	80.4	40	2.61×10^{-5}		318.2	70	2.39×10^{-3}		450.0	60	2.54×10^{-3}
	84.4	45	5.21×10^{-5}		344.6	75	2.95×10^{-3}		483.8	65	3.09×10^{-3}
	89.0	50	5.94×10^{-5}		372.1	80	3.58×10^{-3}		517.8	70	3.75×10^{-3}
	94.7	55	7.44×10^{-5}		394.3	85	4.36×10^{-3}		555.5	75	4.57×10^{-3}
	99.8	60	9.67×10^{-5}		416.7	90	5.44×10^{-3}		586.3	80	5.59×10^{-3}
	106.5	65	1.12×10^{-4}		444.0	95	6.84×10^{-3}		627.2	85	6.64×10^{-3}
	113.7	70	1.33×10^{-4}	0.8757	122.0	20	3.26×10^{-4}		666.7	90	7.89×10^{-3}
	118.4	75	1.64×10^{-4}		152.0	25	4.21×10^{-4}	1.001	334.0	20	3.92×10^{-4}
	124.0	80	2.23×10^{-4}		180.4	30	5.38×10^{-4}		378.6	25	4.63×10^{-4}
	129.0	85	2.89×10^{-4}		212.4	35	6.97×10^{-4}		422.2	30	5.97×10^{-4}
	132.6	90	3.44×10^{-4}		249.0	40	8.89×10^{-4}		471.7	35	7.76×10^{-4}
	137.0	95	4.44×10^{-4}		273.4	45	1.14×10^{-3}		513.1	40	1.05×10^{-3}
0.643	100.0	40	2.49×10^{-4}		319.6	52.5	1.77×10^{-3}		564.4	45	1.31×10^{-3}
	143.9	50	4.06×10^{-4}		335.0	55	1.84×10^{-3}		620.0	50	1.99×10^{-3}
	168.8	60	6.17×10^{-4}		350.6	57.5	2.10×10^{-3}		701.4	60	2.78×10^{-3}
	180.3	65	7.88×10^{-4}		363.2	60	2.35×10^{-3}		748.3	65	3.48×10^{-3}
	194.8	70	9.77×10^{-4}		397.4	65	2.83×10^{-3}		789.0	70	4.18×10^{-3}
	216.7	75	1.23×10^{-3}		413.1	67.5	3.11×10^{-3}		839.5	75	4.97×10^{-3}
	232.3	80	1.54×10^{-3}		431.2	70	3.50×10^{-3}		887.3	80	5.94×10^{-3}
	247.3	85	1.84×10^{-3}		444.6	72.5	3.88×10^{-3}		930.3	85	7.12×10^{-3}
	267.0	90	2.37×10^{-3}		460.4	75	4.17×10^{-3}		975.7	90	8.41×10^{-3}
	272.2	95	2.95×10^{-3}		493.2	80	4.97×10^{-3}		1020.5	95	9.93×10^{-3}
0.803	69.5	20	2.03×10^{-4}		524.1	85	6.21×10^{-3}	1.053	500.0	20	6.11×10^{-4}
	93.9	25	2.55×10^{-4}		557.9	90	7.36×10^{-3}		605.0	30	9.91×10^{-4}
	119.7	30	3.77×10^{-4}		588.4	95	8.83×10^{-3}		726.8	40	1.43×10^{-3}
	144.3	35	4.58×10^{-4}	0.9147	158.0	20	3.43×10^{-4}		836.3	50	2.22×10^{-3}
	168.4	40	6.09×10^{-4}		196.4	25	4.33×10^{-4}		890.9	55	2.67×10^{-3}
	194.6	45	7.67×10^{-4}		237.5	30	5.78×10^{-4}		946.8	60	3.21×10^{-3}
	215.0	50	9.83×10^{-4}		268.3	35	7.24×10^{-4}		999.1	65	3.90×10^{-3}
	244.7	55	1.23×10^{-3}		298.8	40	9.18×10^{-4}		1053.2	70	4.75×10^{-3}
	275.1	60	1.53×10^{-3}		380.0	50	1.72×10^{-3}		1105.4	75	5.71×10^{-3}
	294.7	65	1.91×10^{-3}		394.0	52.5	1.83×10^{-3}		1156.5	80	6.77×10^{-3}
					412.0	55	2.03×10^{-3}				

Table II. Solubility of Anthracene in Carbon Dioxide at 40 °C[a]

	C			C	
P, bar	our data	from ref *11*	P, bar	our data	from ref *11*
100	1.67	3.01	150	3.40	4.18
110	2.13	3.12	175	3.82	4.87
125	2.69	3.76	200	4.07	5.87
135	3.11	3.96			

within 20%. This is because of uncertainties as to the value of the molar absorption coefficient, ϵ. IR absorption measurements of vapor anthracene in equilibrium with the solid phase provided us with $\epsilon = 200 \pm 20$ L cm^{-1} mol^{-1}. Because vapor concentration of anthracene is very small at room temperature (10), the calibration measurements were taken at elevated temperatures varying from 120 to 150 °C. At these temperatures, condensation of anthracene on the windows was a serious problem, so the cell, 150 mm long, was equipped with double KBr windows. Since ϵ is proportional to the transition dipole moment which is sensitive to intermolecular interactions, ϵ may vary with solvent. For example, we found ϵ of the C–H band of anthracene to be 230 ± 10 and 205 ± 9 L cm^{-1} mol^{-1}, for CS_2 and CCl_4 solutions, respectively. We found our data to be in good agreement with the solubilities of anthracene in CO_2 published by Rossling and Franck (*10*) (as illustrated in Figure 3) for the molar absorption coefficient $\epsilon = 180$ L cm^{-1} mol^{-1}. All the calculations of anthracene concentration in CO_2 were performed by using eq 1 assuming $\epsilon = 180$ L cm^{-1} mol^{-1}. Since the ϵ may change with temperature and pressure and also with anthracene concentration in solutions, we have examined the C–H mode molar absorption coefficient of anthracene under various conditions in CCl_4 solutions. No trend has been observed because the data were scattered within the estimated 4% experimental error. On the basis of these observations we assumed that the ϵ in CO_2 solutions was constant at the pressures and temperatures studied.

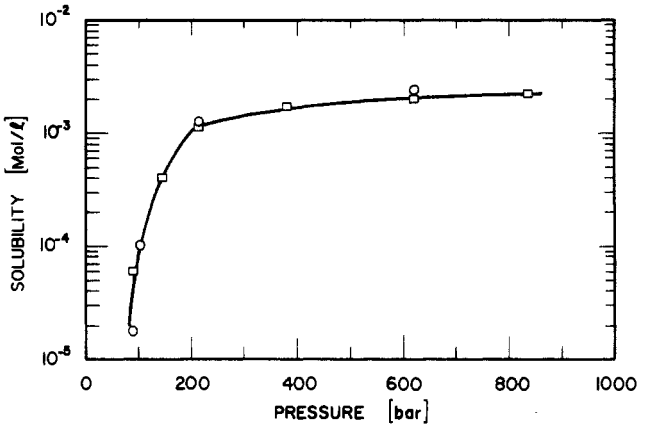

Figure 3. Solubilities of anthracene in carbon dioxide at 50 °C. Squares, this study; circles, Rossling and Franck data (*10*).

Comparison of our data with other reported solubility data (*11*) obtained by using the flow technique is not as satisfactory. Kwiatkowski et al. (*11*) found concentrations of anthracene in CO_2 to be larger than those cited in this paper by about 30% (compare Table II), and these discrepancies cannot be attributed to inaccuracies in determining the ϵ values. It is worth noting that the flow technique used by Kwiatkowski et al. (*11*) is not well suited for measurements of concentration at low solubilities on the order of 10^{-5} mole fraction, in contrast to the FTIR absorption method employed in this study.

It is useful to present the concentration data, C, in the form of enhancement factor C/C^0, where C^0 is the vapor concentration in equilibrium with solid phase (C^0 values were found in Table 2 of ref *10*). After a steep increase the enhancement exceeds a value of 10^5 at 40 °C and 10^4 at 95 °C (compare Figure 4). Although the absolute solubilities increase with

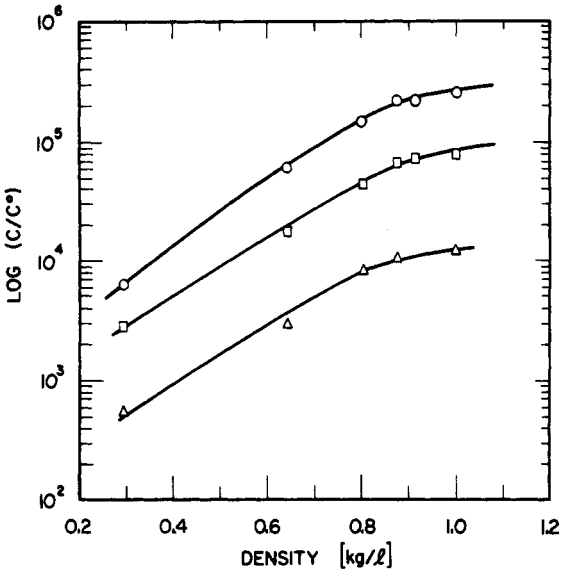

Figure 4. Enhancement factor, C/C^0, for the anthracene–CO_2 system at different temperatures: O, 40 °C; □, 60 °C; △, 95 °C.

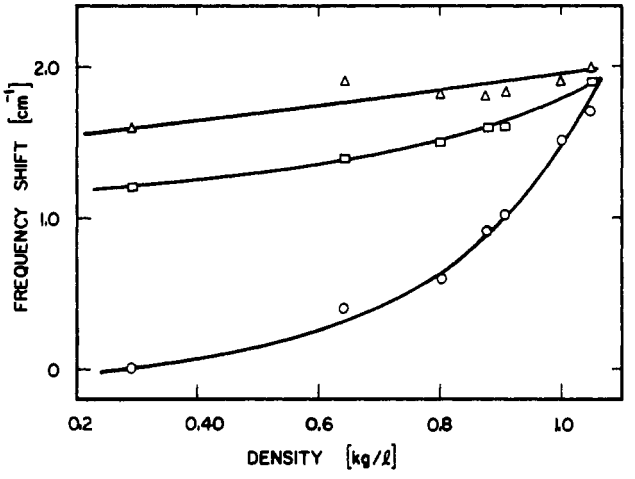

Figure 5. Frequency shift of the maximum of the C–H band of anthracene as a function of density: △, data taken at 95 °C; □, 60 °C; O, 40 °C.

increasing temperature the enhancement factor declines at higher temperatures. At low pressures the enhancement factor increases linearly with solvent density to about 0.9 kg/L and later a saturation is observed. A further rise of solvent density does not affect the enhancement factor. A similar observation was reported previously by Rossling and Franck (*10*).

In Figure 5 we present frequency shift data for three representative temperatures. With increasing temperature and/or pressure the C–H band of anthracene shifts to higher frequency. To the best of our knowledge, this blue shift is characteristic for repulsive forces dominating in the intermolecular interactions (*14*, *15*). This observation is limited to the C–H vibrations located in the plane of the anthracene molecule, and therefore does not preclude the possibility that attractive forces dominate the interactions between CO_2 and the π electron system of anthracene causing the increased solubility. Additional experiments focusing on frequency shifts of ring vibrations of anthracene are now in progress.

Acknowledgment

We thank Dr. M. Bradley for his help in designing the high-pressure IR cell.

Registry No. CO_2, 124-38-9; anthracene, 120-12-7.

Literature Cited

(1) Vitzthum, O.; Hubert, P. German Patent 2 357 590, 1975.
(2) Modell, M.; de Filippi, R. P.; Krukonis, V. J. Presented at the National Meeting of the American Chemical Society, Miami, FL, Sept 14, 1978.
(3) Zhuze, T. P. *Petroleum* **1960**, *23*, 298.
(4) McHugh, M.; Mallett, M.; Kohn, J. Presented at the Annual AIChE Meeting, New Orleans, LA, 1981.
(5) Krukonis, V. J.; Kurnik, R. T. *J. Chem. Eng. Data* **1985**, *30*, 247.
(6) Paulaitis, M. E.; Krukonis, V. J.; Kurnik, R. T.; Reid, R. C. *Rev. Chem. Eng.* **1983**, *1*, 179.
(7) Kurnik, R. T.; Holla, S. J.; Reid, R. C. *J. Chem. Eng. Data* **1981**, *26*, 47.
(8) Van Leer, R. A.; Paulaitis, M. E. *J. Chem. Eng. Data* **1980**, *25*, 257.
(9) Jonas, J.; Lamb, D. Presented at the ACS Symposium on Chemistry and Processing in Supercritical Fluids, at the 190th American Chemical Society National Meeting, Chicago, IL, Sept 9, 1985.
(10) Rossling, G. L.; Franck, E. U. *Ber. Bunsenges. Phys. Chem.* **1983**, *87*, 882.
(11) Kwiatkowski, J.; Lisicki, Z.; Majewski, W. *Ber. Bunsenges. Phys. Chem.* **1984**, *88*, 865.
(12) Zerda, T. W.; Hacura, A.; Zerda, J.; Kluk, E. *Acta Phys. Polon.* **1977**, *A54*, 55.
(13) Newitt, D. M.; Pai, M. U.; Kuloor, N. R.; Huggill, J. A. *Thermodynamic Functions of Gases*; Din, F., Ed.; Butterworths: London, 1962.
(14) Schindler, W.; Zerda, T. W.; Jonas, J. *J. Chem. Phys.* **1984**, *81*, 4306.
(15) Schweizer, K. S.; Chandler, D. *J. Chem. Phys.* **1982**, *76*, 2296.

Received for review October 17, 1985. Accepted December 4, 1985. This study has been partially supported by the Department of Energy under Grant No. DOE DEFG 22-82 PC 50800.